15TH IEA HEAT PUMP CONFERENCE
MAY 26–29, 2026 | HOFBURG
VIENNA 2026
DECARBONISATION THROUGH INNOVATION

Simulation of Ground Source Heat Pump Systems with On/Off Control: Evaluating Part-Load Degradation in Single and Double U-Tube Borehole Configurations

Seyedeh Mahya Mozafary[a,*], Alan S. Fung[a], Wey H. Leong[a]

[a]Toronto Metropolitan University, 350 Victoria Street, Toronto, M5B 2K3, Canada

Abstract

As global demand for sustainable heating and cooling solutions intensifies, ground source heat pump (GSHP) systems are increasingly vital for decarbonizing thermal energy. This study presents a simulation model of GSHP systems integrating single and double U-tube borehole heat exchangers (sBHE and dBHE) with a fixed capacity heat pump operating under on/off control and part-load cycling. Using an implicit finite-difference scheme and thermal resistance network, the model captures unsteady heat transfer in the ground and borehole over time. A minute-based simulation framework enables detailed evaluation of system behaviour, particularly in response to fluctuating building loads.

Ten cases are examined under identical material, geometric, and boundary conditions, while varying the borehole configuration, depth, and fluid mass flow rate. The novel aspect of this study is the inclusion of an adjusted part-load factor (PLF) that accounts for off-cycle power use, minimum runtime constraints, and degradation of efficiency under part load.

PLF adjustment consistently lowers the performance of a GSHP system with reference to the theoretical case without PLF adjustment. On average, the heating coefficient of performance (COP) declines by 6.7-9.5%, the cooling COP decreases by 7.4-9.9%. The effective heat transfer between the heat pump and the borehole is reduced, with seasonal-average fluid temperature difference and corresponding heat exchange per unit borehole length decreasing by approximately 8–11% in heating and 5–8% in cooling. Meanwhile, total compressor work increases by 4-6.9% and overall runtime rises by 5.9-6.8%, reflecting the longer operational periods required under part-load cycling conditions with PLF adjustment.

Keywords: ground source heat pump (GSHP); single U-tube borehole heat exchanger (sBHE); double U-tube borehole heat exchanger (dBHE); fixed-capacity heat pump; on/off operation; part-load modeling

1. Introduction

Global energy investment is undergoing a profound transformation. The International Energy Agency (IEA) projects that capital flows to the energy sector will reach US$ 3.3 trillion in 2025, with US$ 2.2 trillion directed toward renewables, grids, storage, and efficiency, double the amount allocated to fossil fuels [1]. At the same time, the IEA anticipates a rapid increase in cooling demand, with the global number of air-conditioning units expected to rise from 1.6 billion in 2018 to 5.6 billion by 2050, demonstrating the urgent need for energy-efficient HVAC solutions [2].

GSHPs represent one of the most promising options for sustainable heating and cooling. Because the ground maintains a nearly constant temperature throughout the year, GSHPs achieve higher COPs than air-source systems, reducing electricity consumption for both heating and cooling [3]. Although they currently comprise a smaller share of global heat-pump installations, their adoption is accelerating in regions such as Sweden and China, where they provide both energy savings and air-quality improvements despite higher upfront costs [3].

Several field and simulation studies have explored the operational efficiency of GSHP systems with and without partial-load conditions. Kim et al. [4] monitored a vertical water-to-refrigerant GSHP installed in a Korean school, consisting of dual compressors (inverter-type and fixed-speed). They found that the system operated primarily under partial-load conditions, averaging 61% of its capacity in cooling and 51% in heating, and achieved high COPs (6.0–10.9) due to the inverter compressor's ability to modulate operation and maintain stable source and sink temperatures. Daily electricity consumption was reduced by 44–51 kWh compared with an equivalent air-source system. Similarly, García-Céspedes et al. [5] characterized efficiency losses in a double parallel-stage GSHP equipped with fixed-speed compressors operating under real partial-load conditions. They reported that cycling reduced COP by up to 9%, while the effective heating and cooling capacities declined by approximately 20% and 24%, respectively. The study further identified a progressive annual decline in COP, demonstrating the need to account for part-load losses and long-term degradation in GSHP performance assessment.

On the modeling side, Huang et al. [6] developed a mechanism-based TRNSYS simulation to examine long-term thermal degradation in a continuously operating GSHP. Over 20 years, ground temperature (GT) rose by more than 12°C, leading to a nearly linear COP decline of 0.038 per 1°C rise in GT. Their results revealed a 11.3% efficiency loss over two decades, primarily due to thermal-boundary shifts, providing a valuable baseline for distinguishing thermally induced degradation from that caused by part-load cycling.

Control strategy has emerged as another key determinant of GSHP performance. Madani et al. [7] compared three on/off control techniques: constant hysteresis, floating hysteresis, and the degree-minute method, and demonstrated that dynamic, adaptive control minimizes compressor cycling and energy consumption. The degree-minute method achieved the lowest annual energy use and highest seasonal performance factor (SPF), while fixed hysteresis produced frequent short cycling and unstable supply temperatures. Xia et al. [8] advanced this understanding experimentally by developing a model-based optimization strategy for GSHP systems with variable-speed pumps. Their hybrid optimization algorithm combined a performance map with exhaustive search to identify optimal differential-pressure set-points, achieving 8–9% energy savings compared with conventional rule-based control.

Building on these studies, Noye et al. [9] reviewed advanced GSHP control methods, ranging from rule-based to artificial-intelligence-based approaches, and emphasized that fixed on/off control governed by static set-points causes excessive cycling, reduced COP, and mechanical wear. They argued for adaptive supervisory control frameworks that integrate model-predictive or reinforcement-learning techniques to limit cycling and stabilize performance, highlighting the same operational inefficiencies that motivate explicit PLF modeling.

In parallel, Mahmoudi Majdabadi and Koohi-Fayegh [10] proposed a semi-analytical dynamic GSHP model for medium- and long-term performance assessment. Their framework couples a detailed thermodynamic heat-pump model with an analytical ground-heat-exchanger representation and explicitly includes on/off cycling losses through a PLF correction derived from the Henderson and Rengarajan model. Sensitivity analysis confirmed that higher cycling frequencies correlate with measurable COP reduction. Although their main focus was on ground-temperature variation, their incorporation of PLF-based degradation places their work among the few recent studies that quantitatively integrate cycling-related efficiency losses into GSHP simulation.

Together, these studies illustrate the evolution of GSHP research, from field-based performance monitoring [4, 5], to long-term thermal modeling [6], control-strategy optimization [7-9], and recent semi-analytical modeling that embeds part-load and cycling effects [10]. However, most existing work either assumes continuous operation or represents part-load effects through empirical corrections rather than explicit on/off cycling dynamics. The present study builds upon these findings by developing a detailed time-resolved GSHP simulation that directly quantifies COP degradation due to PLF adjustments under realistic cycling conditions, thereby addressing an unresolved gap in long-term performance modeling.

2. Methodology

Building upon the previously validated finite-difference borehole heat exchanger (BHE) model by Kerme et al. [11, 12], this study develops a dynamic simulation framework for GSHP systems operating under on/off control and part-load cycling. The GSHP system model consists of the BHE model, a fixed-capacity heat pump with known performance curves, a set of hourly heating and cooling loads of a house, and a part-load degradation model which incorporates an on/off and part-load cycling operation of the heat pump with an adjusted PLF.

The formulation of the BHE model is based on transient heat conduction and energy rate balance principles, assuming a homogeneous and isotropic ground. The numerical formulation of the BHE model follows a control-volume–based energy balance for the circulating fluid, grout, and surrounding soil domain. Transient heat conduction in the radial direction and convective heat transfer between the working fluid and borehole wall are considered. The governing energy balance equations for the downward- and upward-flowing fluid legs, grout, and soil nodes are spatially discretized using a finite-difference scheme and solved using a Crank–Nicolson implicit formulation, ensuring numerical stability and second-order temporal accuracy.

Detailed derivations, numerical implementation, and validation of the BHE and GSHP models are provided in Refs. [11-14].

In this paper, two modeling approaches are studied and compared:

- an adjusted PLF model, which accounts for degradation effects due to part-load cycling, off-cycle losses, and minimum runtime limits, with part-load heat pump performance during the actual runtime of the GSHP system; and
- a non-adjusted PLF model, assuming ideal steady-state heat pump performance during the theoretical runtime of the GSHP system.

A total of ten simulation cases were defined under identical geometric, material, and boundary conditions, varying borehole configuration (single vs. double U-tube), borehole depth, and total fluid mass flow rate to isolate the effects of PLF correction on system behavior and efficiency.

All material properties are assumed constant. The parameters used for all cases are summarized in Table 1. The selected values for key parameters, including ground/soil thermal conductivity, shank spacing, and borehole depth, are based on prior sensitivity analyses [12,13].

Table 1. Input parameters used in the simulation

Parameter	Symbol	Value
Half shank spacing of U-tube (m)	d	0.08697
Borehole radius (m)	r_b	0.1
U-tube pipe inner radius (m)	r_{pi}	0.01103
U-tube pipe outer radius (m)	r_{po}	0.01303
U-tube pipe thermal conductivity (W/m·K)	k_p	0.4
Soil thermal conductivity (W/m·K)	k_s	2.5
Soil specific heat capacity (J/kg·K)	C_s	2016
Soil density (kg/m³)	ρ_s	2000
Grout thermal conductivity (W/m·K)	k_b	0.5
Grout specific heat capacity (J/kg·K)	C_b	2200
Grout density (kg/m³)	ρ_b	1800
Fluid thermal conductivity (W/m·K)	k_f	0.6
Fluid specific heat capacity (J/kg·K)	C_f	4183
Fluid density (kg/m³)	ρ_f	997
Fluid viscosity (Pa·s)	μ_f	0.0008905
Undisturbed ground temperature (°C)	T_g	10

The heat pump is modeled as a fixed-capacity unit operating under on/off cycling. The performance representation corresponds to a nominal 3.5-ton (≈12.3 kW) heat pump operating at a water flow rate of 10 GPM (gallons per minute) and an air flow rate of approximately 1200–1400 CFM (cubic feet per minute). At the nominal rating conditions, the heating coefficient of performance (COP) is approximately 3.5 at an entering water temperature (EWT) of 10 °C, while the cooling performance corresponds to an energy efficiency ratio (EER), defined as the ratio of cooling capacity to electrical input power, of approximately 13.7 at an EWT of 21.1 °C, with a nominal capacity of about 12.3 kW. Heating and cooling capacities, as well as COP/EER variations with EWT, were extracted from the published performance data reported by Kavanaugh [15], and the coefficients in Eqs. (1–4) were obtained by curve-fitting these data and subsequently scaled to match the building design load**.**

$$COP_H = 0.0011T_{EWT}^2 + 0.0225T_{EWT} + 3.1716 \quad (1)$$

$$COP_C = -0.0765T_{EWT} + 5.6251 \quad (2)$$

$$\dot{Q}_H = 105.5T_{EWT} + 3535.7 \quad (3)$$

$$\dot{Q}_C = -0.8445T_{EWT}^2 + 18.1826T_{EWT} + 4300.8 \quad (4)$$

where COP_H and COP_C are the heating and cooling coefficients of performance of the heat pump, respectively; $\dot{Q}_H$ and $\dot{Q}_C$ are the heating and cooling capacities of the heat pump (W); and T_{EWT} is the entering water temperature to the heat pump (°C).

For the case without PLF adjustment, i.e. without part-load degradation, the theoretical PLF (PLF_t) is simply equal to the part load ratio (PLR):

$$PLF_t = PLR \equiv \frac{Hourly\ Building\ Load}{Available\ Heat\ Pump\ Capacity} \quad (5)$$

where PLR is the part-load ratio defined as the ratio of the hourly building load to the available heat pump capacity; PLF_t is the theoretical part-load factor assuming no cycling degradation.

To account for efficiency loss during cycling, the PLF is applied using a standard HVAC correlation, which introduces a correction dependent on the PLR [16]:

$$PLF = 1 - C_d(1 - PLR) \quad (6)$$

where PLF is the cycling-degraded part-load factor; C_d is the degradation coefficient accounting for on/off cycling losses; this study, a degradation coefficient of $C_d = 0.081$ is adopted, corresponding to a good residential heat pump with a maximum cycling rate of $N_{\max} = 3$ cycles per hour. This value was obtained by calibrating the part-load factor formulation to match with the recommended energy input ratio (EIR) curves for good residential heat pumps reported in the U.S. Department of Energy–2 (DOE-2) [17].

The adjusted PLF (accounting for off-cycle power consumption with an assumption of 1% of the on-cycle power consumption, i.e. $p_r = 0.01$) is computed as [18]:

$$PLF_A = \frac{PLR}{PLR/PLF + (1 - PLR/PLF)p_r} \quad (7)$$

where p_r is the ratio of off-cycle to on-cycle power consumption.

The effective COP becomes:

$$COP_{eff} = COP_{rated} \times PLF_A \quad (8)$$

where COP_{eff} is the effective coefficient of performance accounting for part-load degradation, and COP_{rated} is the rated heat pump COP obtained from the manufacturer-based performance correlations.

The minimum on-time of the GSHP system can be calculated as follows [19]:

$$t_{ON,min} = \frac{3600}{4N_{max}} \tag{9}$$

where $t_{ON,min}$ is the minimum on-time of the GSHP system within one hour (s), and N_{max} is the maximum number of compressor on/off cycles per hour. N_{max} = 3 cycles per hour is used in the present study, which results in $t_{ON,min}$ = 300 s or 5 minutes.

The inclusion of this degradation model enables the simulation to capture losses due to frequent cycling, short runtime inefficiencies, and residual power consumption during off periods; effects that are otherwise ignored in idealized GSHP models.

Table 2 lists ten cases which are studied to isolate the influence of borehole configuration, total fluid mass flow rate, and borehole depth with (PLF_A) and without (PLF_t) part-load degradation adjustment. For the cases of dBHE, each U-tube assumes half of the total fluid mass flow rate. Each case is simulated under identical annual building load conditions to evaluate the thermal and operational effects of part-load degradation.

Figure 1 shows the hourly building load profile of a house over one year, with negative and positive values representing heating and cooling loads, respectively. The annual energy demands and peak loads are:

- Annual heating demand: 7037 kWh
- Annual cooling demand: 4551 kWh
- Peak heating load: –3504 W
- Peak cooling load: 3459 W

The ratio of annual heating to cooling demand is 1.55, which implies a heating-dominated building load profile. Nevertheless, the corresponding ground thermal balance may differ due to the influence of heat pump performance, particularly the heating and cooling COPs. As shown in Table 3, the annual heat rejected to the ground exceeds the heat extracted, indicating a cooling-dominated geo-exchange behavior despite the heating-dominated building load.

Table 2. Specific input parameters used in the simulation

Case	BHE type	Borehole depth (m)	Total mass flow rate (kg/s)	PLF
Base 1	sBHE	75	0.2	Adjusted
Base 2	dBHE	75	0.2	Adjusted
Case 1	sBHE	75	0.2	Not adjusted
Case 2	dBHE	75	0.2	Not adjusted
Case 3	dBHE	75	0.1	Adjusted
Case 4	dBHE	75	0.1	Not adjusted
Case 5	dBHE	50	0.2	Adjusted
Case 6	dBHE	50	0.2	Not adjusted
Case 7	dBHE	60	0.2	Adjusted
Case 8	dBHE	60	0.2	Not adjusted

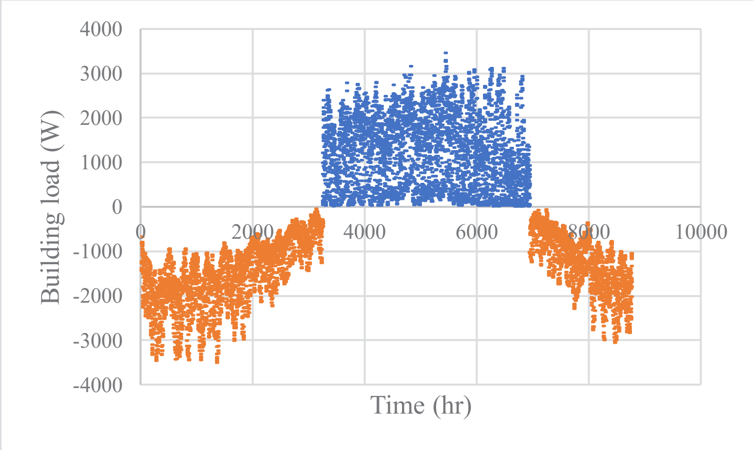

Figure 1. The building's hourly load profile over one year.

Loads are applied as dynamic inputs (in W) representing realistic residential operation. In each hour, the building heating or cooling load is assumed to be constant, and the actual runtime (in s) of the system is calculated as:

$$t_{ON,a} = \frac{3600 \times PLR}{PLF_A} \tag{10}$$

And the remaining time of the hour will be off-time. Otherwise, for the case without PLF adjustment, the GSHP system will run on the theoretical runtime (s) within an hour as follows:

$$t_{ON,t} = 3600 \times PLF_t \tag{11}$$

where $t_{\mathrm{ON,a}}$ is the actual compressor runtime within one hour accounting for part-load degradation (s), and $t_{\mathrm{ON,t}}$ is the theoretical runtime assuming ideal operation without cycling losses (s). If $t_{\mathrm{ON,a}} < t_{ON,min}$, i.e. less than 5 minutes, it will be set equal to $t_{ON,min}$, i.e. $t_{\mathrm{ON,a}} = t_{ON,min}$.

A Crank–Nicolson implicit finite-difference scheme is implemented for temporal discretization with a time step of 60 s and an annual simulation period of 8760 h. The radial and axial mesh sizes are chosen to ensure convergence and numerical stability.

Boundary conditions:

- Constant temperature of 10°C at the far-field boundary of the BTES;
- Adiabatic top and bottom boundaries of the BTES;
- Continuity of heat flux at all interfaces.

Key performance metrics recorded include:

- Average heat pump fluid temperature difference (ΔT)
- Annual extracted/rejected heat (Q_{ext}/Q_{rej}) from/to BTES
- Effective heat-pump COP (heating/cooling) during the actual runtime
- Total actual runtime of the system
- Total compressor work
- Total ground-loop pump work

3. Results and Discussion

The results of the simulations are summarized in Table 3, which reports the key seasonal and annual performance metrics for all cases. Heating- and cooling-season results are presented separately where relevant, while annual values are reported for cumulative energy consumption and total system runtime. In addition to effective coefficients of performance, annual heat extraction and rejection, and electrical energy consumption, the seasonal-average fluid temperature difference (ΔT) is included as a representative thermal indicator linking part-load cycling to heat transfer effectiveness. Complementary figures (Figs. 2–10) illustrate both seasonal and annual trends in system performance.

Table 3. Simulation results

Parameter	Base 1	Base 2	Case 1	Case 2	Case 3	Case 4	Case 5	Case 6	Case 7	Case 8
ΔT (Heating) (°C)	2.91	3.1	3.25	3.68	6.48	7.28	2.98	3.33	3.08	3.46
ΔT (Cooling) (°C)	5.70	5.97	6.09	6.61	12.08	12.94	5.98	6.30	5.94	6.36
Q_{ext} (Heating) (kWh)	-4709.44	-4820.00	-4860.53	-5080.78	-4846.89	-4992.63	-4751.16	-4895.15	-4784.34	-4932.60
Q_{rej} (Cooling) (kWh)	5530.10	5636.16	5450.75	5698.85	5681.77	5613.51	5656.58	5576.05	5643.54	5568.95
$COP_{eff,H}$ (Heating)	3.09	3.13	3.31	3.46	3.13	3.37	3.08	3.30	3.10	3.33
$COP_{eff,C}$ (Cooling)	3.87	4.11	4.18	4.56	4.14	4.47	3.85	4.17	3.98	4.31
Total runtime (h)	3058.72	2916.34	2887.51	2735.77	2891.38	2707.89	3038.49	2861.50	2974.77	2795.20
Total compressor work (kWh)	3529.27	3360.71	3324.82	3223.48	3329.90	3115.14	3494.97	3283.82	3426.09	3214.45
Total ground-loop pump work (kWh)	16.68	4.81	15.74	4.62	0.74	0.69	3.35	3.15	3.93	3.69

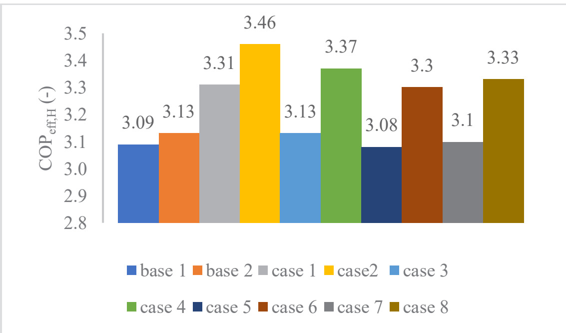

Figure 2. $COP_{eff,H}$ averaged over the heating season for all cases.

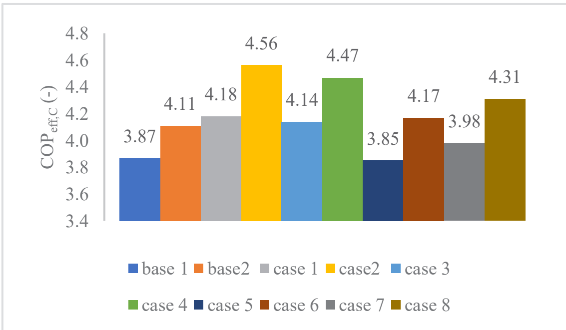

Figure3. $COP_{eff,C}$ averaged over the cooling season for all cases.

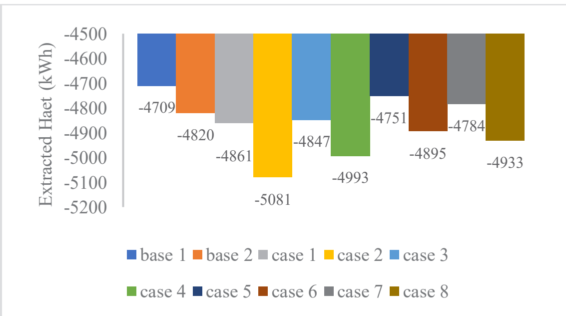

Figure 4. Q_{ext} in the heating season for all cases.

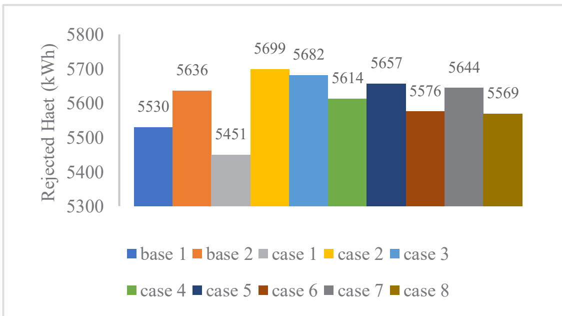

Figure 5. Q_{rej} in the cooling season for all cases.

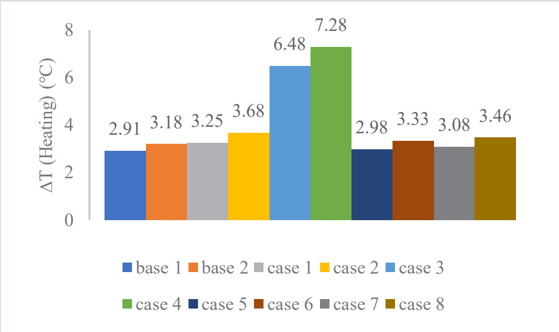

Figure 6. Fluid temperature difference in the heating season. averaged over the season for all cases.

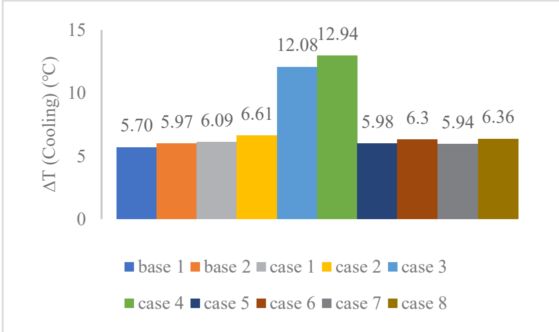

Figure 7. Fluid temperature difference in the cooling season. average over the season for all cases.

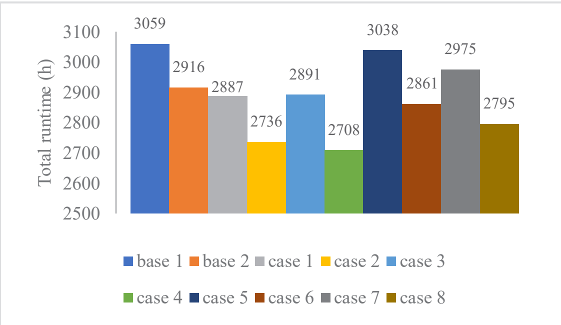

Figure 8. Total runtime over a year for all cases.

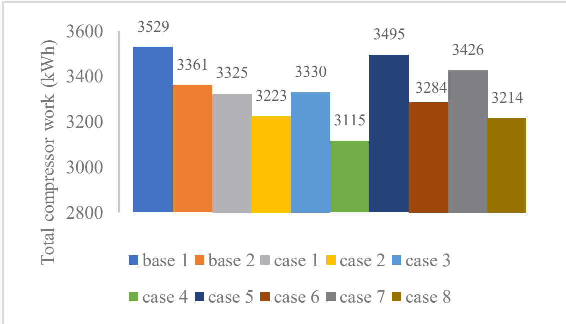

Figure 9. Total compressor work over a year for all cases.

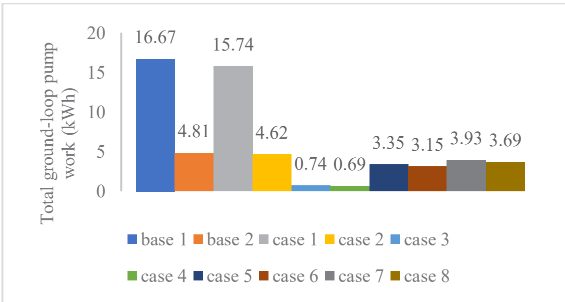

Figure 10. Total ground-loop pump work over a year for all cases.

Overall, incorporating part-load degradation through the adjusted PLF consistently alters GSHP performance across all configurations. Relative to the non-adjusted cases, the PLF-adjusted cases exhibit reduced effective heat transfer between the heat pump and the borehole, reduced seasonal efficiency, and increased annual operating time. These changes arise from start-up transients, off-cycle losses, and reduced effective heat transfer per unit runtime during on/off cycling.

A clear manifestation of this behavior is observed in the seasonal-average fluid temperature difference. Across all cases, ΔT decreases by approximately 10–14% in heating and 5–10% in cooling when PLF adjustment is applied (Table 3). Because mass flow rate and fluid properties remain unchanged between adjusted and non-adjusted cases, the reduction in ΔT directly indicates reduced instantaneous heat exchange between the heat pump and the borehole heat exchanger. For example, comparing Base 1 and Case 1 (single U-tube with identical borehole geometry), the heating-season ΔT decreases by approximately 11%, leading to a reduction in total heat extraction of about 4%, despite a longer operating duration in the PLF-adjusted case. This confirms that longer runtime does not fully compensate for the reduced heat-transfer effectiveness introduced by cycling losses.

From an energy perspective, total heat extraction in heating decreases for all PLF-adjusted cases by approximately 3–5%, while total heat rejection in cooling generally increases by about 1–2%. The increase in cooling-season heat rejection occurs because the extended runtime outweighs the reduced instantaneous heat-transfer effectiveness. An exception is observed for the Base 2–Case 2 configuration, where total heat rejection decreases slightly, indicating that in this case, the reduction in effective heat exchange is not fully offset by increased runtime. These trends demonstrate that part-load degradation affects heating and cooling operation differently, with heating performance being more sensitive to reduced heat-transfer effectiveness.

The impact of part-load cycling is also evident in the effective coefficients of performance. Across all configurations, the heating COP decreases by approximately 6–10%, while the cooling COP decreases by 7–10% under PLF adjustment (Table 3 and Figs. 2–3). Although PLF adjustment leads to slightly higher entering water temperatures during the heating season, which would normally benefit COP, the negative effects of cycling losses dominate. This indicates that part-load degradation has a stronger influence on system efficiency than modest improvements in source temperature. The reduced effective COPs reflect the combined influence of inefficient compressor restarts, off-cycle standby losses, and unsteady operation inherent to fixed-capacity systems under on/off control.

As a consequence of reduced effective efficiency, electrical energy consumption increases. Total compressor work rises by approximately 4–7% across all cases, while total ground-loop pump work increases modestly but consistently. These increases are directly associated with longer operating durations required to meet the same annual building loads under degraded part-load conditions. Annual system runtime increases by approximately 6–7%, confirming that PLF adjustment primarily manifests as extended operation at lower instantaneous efficiency rather than large shifts in peak performance (Figs. 8–10).

The comparative analysis of system configurations highlights design features that mitigate part-load degradation. Configurations with deeper boreholes exhibit more stable ground temperatures, reduced sensitivity to cycling losses, and higher effective COPs in both heating and cooling. Similarly, double U-tube configurations, which provide lower effective borehole thermal resistance, maintain more stable operating conditions and reduce compressor strain. Reduced mass flow rate also shows modest benefits in selected cases by increasing fluid residence time in the BHE for longer heat exchange time with smaller heat capacity rate resulting in more favourable entering water temperature for heat pump, provided that turbulent flow conditions are maintained [13]. For instance, Case 3 achieves COPs comparable to or slightly higher than Base 2, despite operating at half the mass flow rate, while maintaining turbulent flow in the U-tubes, with Reynolds numbers of approximately 3241 and 6481 for Case 3 and Base 2, respectively, both exceeding the critical value of 2300.

4. Conclusion

This study developed a minute-based dynamic simulation model for GSHP systems with a fixed-capacity heat pump operating under on/off control and a BTES containing sBHE or dBHE. By incorporating an adjusted PLF to mimic the effects of real-world cyclic operation, the model accounts for degradation due to part-load cycling, minimum runtime constraints, and off-cycle power consumption, factors often neglected in simulations.

Across ten simulated cases, the inclusion of PLF adjustment consistently reduced both heating and cooling COPs by approximately 6–10%, as compared to the non-adjusted cases. Total heat extraction from the BHE is decreased by approximately 3–5%, while the total heat rejection is mainly increased by approximately 1%. The annual compressor work and system runtime are increased by roughly 4–7% and 6-7%, respectively, as the heat pump operated longer to meet the same building loads.

These findings confirm that neglecting part-load degradation can lead to optimistic performance predictions. The PLF-adjusted model provides a more realistic representation of residential-scale GSHP operation under on/off control, thereby improving the reliability of system performance assessment and design. Among the configurations studied, systems employing double U-tube boreholes, deeper borehole depths, and lower total mass flow rates exhibited the most stable operation and the smallest performance degradation under PLF-adjusted conditions. The double U-tube configuration reduces effective borehole thermal resistance and promotes more uniform heat transfer, while increased borehole depth enhances ground thermal capacity and mitigates the adverse effects of cycling.

Future work could focus on extending this approach to variable-speed heat pumps to explore control strategies that enhance long-term operational stability. Present study is only limited to one-year simulations. Multiple-year simulations will be needed to study long-term impact of on/off control and part-load cycling.

Nomenclature

C_d	degradation coefficient (-)
COP_C	rated cooling COP (-)
COP_{eff}	effective COP (-)
$COP_{eff,C}$	effective COP of the cooling season (-)
$COP_{eff,H}$	effective COP of the heating season (-)
COP_H	rated heating COP (-)
COP_{rated}	rated COP of the heat pump (-)
N_{max}	maximum cycle rate (cycles/h)
p_r	fraction of the on-cycle power consumption (-)
PLF	part load factor (-)
PLF_A	adjusted part load factor (-)
PLF_t	Theoretical PLF (-)
PLR	ratio of hourly building load to available heat pump capacity (-)
$\dot{Q}_C$	rated cooling capacity of the heat pump (W)
$\dot{Q}_H$	rated heating capacity of the heat pump (W)
Q_{ext}	total heat extracted from borehole (kWh)
Q_{rej}	total heat rejected to borehole (kWh)
T_{EWT}	entering water temperature (°C)
$t_{ON,a}$	actual runtime (s)
$t_{ON,min}$	minimum on-time of the GSHP system (s)
$t_{ON,t}$	theoretical runtime (s)

Acknowledgements

The authors gratefully acknowledge the financial support provided by the Canada First Research Excellence Fund (CFREF) Volt-Age project and the Natural Sciences and Engineering Research Council (NSERC) of Canada Discovery Grant, which made this research possible. Their contributions have been instrumental in advancing this study, and we sincerely appreciate their support.

References

[1] International Energy Agency, 2025: IEA (2025), World Energy Investment 2025, IEA, Paris https://www.iea.org/reports/world-energy-investment-2025 , Licence: CC BY 4.0

[2] Abdel-Salam, M. R. H., & Zaidi, A. (2021). Field study of cooling performance of two ground-source heat pumps in Canadian single-family houses. Applied Thermal Engineering, 184, 116294. https://doi.org/10.1016/j.applthermaleng.2020.116294

[3] International Energy Agency, 2022: IEA (2022), The Future of Heat Pumps, IEA, Paris https://www.iea.org/reports/the-future-of-heat-pump , Licence: CC BY 4.0

[4] Kim, E., Lee, J., Jeong, Y., Hwang, Y., Lee, S., & Park, N. (2012). Performance evaluation under the actual operating condition of a vertical ground source heat pump system in a school building. Energy and Buildings,50, 16. https://doi.org/10.1016/j.enbuild.2012.02.006

[5] García-Céspedes, J., Arnó, G., Herms, I., & de Felipe, J. J. (2020). Characterisation of efficiency losses in ground source heat pump systems equipped with a double parallel stage: A case study. *Renewable Energy, 147*(Part 2), 2761–2773. https://doi.org/10.1016/j.renene.2019.01.029

[6] Huang, Y., Zhao, Z., & Sun, M. (2025). Performance Degradation of Ground Source Heat Pump Systems Under Ground Temperature Disturbance: A TRNSYS-Based Simulation Study. *Energies*, *18*(15), 3909. https://doi.org/10.3390/en18153909

[7] Madani, H., Claesson, J., & Lundqvist, P. (2013). *A descriptive and comparative analysis of three common control techniques for an on/off controlled ground source heat pump (GSHP) system. Energy and Buildings, 65,* 1–9. https://doi.org/10.1016/j.enbuild.2013.05.006

[8] Xia, L., Ma, Z., McLauchlan, C., & Wang, S. (2017). *Experimental investigation and control optimization of a ground source heat pump system. Applied Thermal Engineering, 127,* 70–80. https://doi.org/10.1016/j.applthermaleng.2017.07.205

[9] Noye, S., Mulero Martinez, R., Carnieletto, L., De Carli, M., & Castelruiz Aguirre, A. (2022). *A review of advanced ground source heat pump control: Artificial intelligence for autonomous and adaptive control. Renewable and Sustainable Energy Reviews, 153,* 111685. https://doi.org/10.1016/j.rser.2021.111685

[10] Mahmoudi Majdabadi, M., & Koohi-Fayegh, S. (2025). A Semi-Analytical Dynamic Model for Ground Source Heat Pump Systems: Addressing Medium- to Long-Term Performance Under Ground Temperature Variations. *Sustainability*, *17*(12), 5391. https://doi.org/10.3390/su17125391

[11] Kerme, E. D., & Fung, A. S. (2020). Transient heat transfer simulation, analysis and thermal performance study of double U-tube borehole heat exchanger based on a numerical heat transfer model. Applied Thermal Engineering,173,*115189*. https://doi.org/10.1016/j.applthermaleng.2020.115189

[12] Kerme, E. D., & Fung, A. S. (2021). Comprehensive simulation based thermal performance comparison between single and double U-tube borehole heat exchanger and sensitivity analysis. Energy and Buildings, 241, 259-281. https://doi.org/10.1016/j.enbuild.2021.110876

[13] Kerme, E. D., Fung, A. S., & Leong, W. H. (2024). Analysis of the Combined Effect of Major Influencing Parameters for Designing High-Performance Single (sBHE) and Double (dBHE) U-Tube Borehole Heat Exchangers. Energies. 17, 2525. https://doi.org/10.3390/en17112525

[14] Mozafary, S. M., Fung, A. S., Leong, W. H., & Kerme, E. D. (2025). Performance comparison of single and double U-tube borehole heat exchangers in ground source heat pump systems. In Proceedings of the CSME-CFDSC-CSR 2025 International Congress (Progress in Canadian Mechanical Engineering, Vol. 8, Montreal, QC, Canada, May 25 – 28, 2025). https://doi.org/10.82417/d25f-gj76

[15] Kavanaugh, S. (1988). Ground and water source heat pump performance and design for southern climates. Energy Systems Laboratory, Texas A&M University. https://hdl.handle.net/1969.1/6518

[16] Parken, W.H., Didion, D. A., Wojciechowshi, P.H., & Chern, L. (1985). Field Performance of Three Residential Heat Pumps in the Cooling Mode. NBSIR 85-3107, report by National Bureau of Standards, sponsored by U.S. Department of Energy for U.S. Department of Commerce, March.

[17] Huang, Y.J., Parker, D.S., Henderson, H.I., Huang, Y.J., & Solar, F. (1999). Residential equipment part load curves for use in DOE-2.

[18] Bonne, U., Patani, A., Jacobson, R. D. & Mueller, D. A. (1980). Electric-Driven Heat Pump Systems: Simulations and Controls II. ASHRAE Transactions. 86(1) LA-80-5 No. 4. pp 687-705.

[19] Henderson, H. I., Rengarajan, K., & Raustad, R. (1991). Measuring Thermostat and Air Conditioner Performance in Florida Homes. Research Report #FSEC-RR-24-91. Florida Solar Energy Center, Cape Canaveral, FL. May.f